NeuroImage: Clinical 31 (2021) 102740

Contents lists available at ScienceDirect

NeuroImage: Clinical

journal homepage: www.elsevier.com/locate/ynicl

Neurofibrillary tau depositions emerge with subthreshold cerebral beta-amyloidosis in down syndrome

Matthew D. Zammit [a,b,*], Dana L. Tudorascu [c], Charles M. Laymon [d,e], Sigan L. Hartley [a], Paul A. Ellison [b], Shahid H. Zaman [f], Beau M. Ances [g], Sterling C. Johnson [h], Charles K. Stone [i], Marwan N. Sabbagh [j], Chester A. Mathis [c], William E. Klunk [c], Ann D. Cohen [c], Benjamin L. Handen [c], Bradley T. Christian [a,b]

[a] University of Wisconsin-Madison Waisman Center, Madison, WI, USA
[b] University of Wisconsin-Madison Department of Medical Physics, Madison, WI, USA
[c] University of Pittsburgh Department of Psychiatry, Pittsburgh, PA, USA
[d] University of Pittsburgh Department of Radiology, Pittsburgh, PA, USA
[e] University of Pittsburgh Department of Bioengineering, Pittsburgh, PA, USA
[f] Cambridge Intellectual Disability Research Group, University of Cambridge, Cambridge, UK
[g] Washington University in St. Louis Department of Neurology, St. Louis, MO, USA
[h] University of Wisconsin-Madison Alzheimer's Disease Research Center, Madison, WI, USA
[i] University of Wisconsin-Madison Department of Medicine, Madison, WI, USA
[j] Cleveland Clinic Nevada, Las Vegas, NV, USA

ARTICLE INFO

Keywords:
Down syndrome
Amyloid
Neurofibrillary tau
Early detection

ABSTRACT

Introduction: Adults with Down syndrome are genetically predisposed to develop Alzheimer's disease and accumulate beta-amyloid plaques (Aβ) early in life. While Aβ has been heavily studied in Down syndrome, its relationship with neurofibrillary tau is less understood. The aim of this study was to evaluate neurofibrillary tau deposition in individuals with Down syndrome with varying levels of Aβ burden.

Methods: A total of 161 adults with Down syndrome (mean age = 39.2 (8.50) years) and 40 healthy, non-Down syndrome sibling controls (43.2 (12.6) years) underwent T1w-MRI, [C-11]PiB and [F-18]AV-1451 PET scans. PET images were converted to units of standardized uptake value ratios (SUVrs). Aβ burden was calculated using the amyloid load metric ($A\beta_L$); a measure of global Aβ burden that improves quantification from SUVrs by suppressing the nonspecific binding signal component and computing the specific Aβ signal from all Aβ-carrying voxels from the image. Regional tau was assessed using control-standardized AV-1451 SUVr. Control-standardized SUVrs were compared across Down syndrome groups of Aβ-negative (A-) ($A\beta_L < 13.3$), subthreshold A+ ($13.3 \leq A\beta_L < 20$) and conventionally A+ ($A\beta_L \geq 20$) individuals. The subthreshold A + group was identified as having significantly higher Aβ burden compared to the A- group, but not high enough to satisfy a conventional A + classification.

Results: A large-sized association that survived adjustment for chronological age, mental age (assessed using the Peabody Picture Vocabulary Test), and imaging site was observed between $A\beta_L$ and AV-1451 within each Braak region ($p < .05$). The A + group showed significantly higher AV-1451 retention across all Braak regions compared to the A- and subthreshold A + groups ($p < .05$). The subthreshold A + group showed significantly higher AV-1451 retention in Braak regions I-III compared to an age-matched sample from the A- group ($p < .05$).

Discussion: These results show that even the earliest detectable Aβ accumulation in Down syndrome is accompanied by elevated tau in the early Braak stage regions. This early detection of tau can help characterize the tau accumulation phase during preclinical Alzheimer's disease progression in Down syndrome and suggests that there may be a relatively narrow window after Aβ accumulation begins to prevent the downstream cascade of events that leads to Alzheimer's disease.

* Corresponding author at: University of Wisconsin-Madison Waisman Center, Madison, WI, USA.
E-mail address: mzammit@wisc.edu (M.D. Zammit).

https://doi.org/10.1016/j.nicl.2021.102740
Received 25 March 2021; Received in revised form 20 May 2021; Accepted 21 June 2021
Available online 24 June 2021

1. Introduction

Adults with Down syndrome are at high risk of developing Alzheimer's disease. Down syndrome is characterized by triplication of chromosome 21, which encodes production of the amyloid precursor protein (APP) and results in early amyloid-β (Aβ) plaque deposition in the brain (Oyama et al., 1994; Rumble et al., 1989). There is a sharp increase in prevalence of Alzheimer's disease dementia after age 50 in Down syndrome (Schupf, 2002), with the average age of dementia onset at 55 years (Strydom et al., 2018). The lifetime risk of developing Alzheimer's disease in Down syndrome is over 90% (McCarron et al., 2017, 2014), with a survival time of ~4 years following a dementia diagnosis (Sinai et al., 2018). Since Alzheimer's disease is the leading cause of death in this population (Hithersay et al., 2019), there is motivation to include individuals with Down syndrome in trials aimed at Alzheimer's disease treatment and prevention, and particularly anti-amyloid interventions.

The progression of Aβ plaques throughout Alzheimer's disease in Down syndrome has been studied extensively. Pittsburgh Compound-B (2-(4′-[11C]methylaminophenyl)-6-hydroxybenzothiazole, [C-11]PiB) is a positron emission tomography (PET) radiotracer that is used for the non-invasive imaging of Aβ plaques in neuronal tissue. Using [C-11]PiB PET, the earliest region of prominent Aβ retention was identified as the striatum (Handen et al., 2012). This striatum-first pattern of Aβ deposition in Down syndrome is consistent with the observations in individuals with autosomal-dominant Alzheimer's disease and APP duplication (Bateman et al., 2012; Klunk et al., 2007; Remes et al., 2008; Villemagne et al., 2009). Similar to late-onset Alzheimer's disease, Down syndrome presents identical patterns of cortical Aβ retention (Annus et al., 2016; Cole et al., 2017; Hartley et al., 2014; Jennings et al., 2015; Landt et al., 2011; Lao et al., 2018, 2016; Mak et al., 2019; Matthews et al., 2016; Rafii et al., 2015, 2017; Sabbagh et al., 2015) and shows longitudinal increases of ~3–4% per year, however with a wide variation in the age of Aβ onset (Lao et al., 2017; Tudorascu et al., 2019; Zammit et al., 2020). In late-onset Alzheimer's disease, striatal Aβ retention is observed much later in the disease progression (Hanseeuw et al., 2018) compared to Down syndrome, indicating that the striatum can be used as an early marker of Alzheimer's disease progression in this population (Cohen et al., 2018). The onset of brain amyloidosis in Down syndrome occurs some 10 to 15 years earlier than in the non-Down syndrome general population and the deposition of amyloid plaques is necessary but not sufficient for onset of cognitive symptoms.

With improvements in PET quantification techniques, emphasis has been placed on early detection of Aβ, specifically at subthreshold detection levels where the total Aβ burden would not satisfy a conventional Aβ-positive (A+) classification. In late-onset Alzheimer's disease studies, subthreshold Aβ change has been linked to early tau change and worsening cognitive performance (Hanseeuw et al., 2019; Landau et al., 2018; Leal et al., 2018). To better characterize subthreshold Aβ change in Down syndrome, our previous work evaluated longitudinal Aβ accumulation during the earliest stages of Aβ accumulation. Aβ accumulation in individuals with Down syndrome at typical subthreshold levels was found to be similar to Aβ accumulation in individuals with Down syndrome with moderate to high Aβ burden. Using the longitudinal Aβ data, a cutoff representing subthreshold A+ was established to distinguish early Aβ accumulators from Aβ-negative (A−) non-accumulators given just a single PET scan (Zammit et al., 2021). The classification of subthreshold A+ was leveraged using longitudinal evaluation with the amyloid load metric ($A\beta_L$). The $A\beta_L$ metric is similar to Centiloids and at the cross-sectional level both measures are highly correlated, but $A\beta_L$ shows improved longitudinal stability due to its suppression of the nonspecific binding signal component of PET images (Whittington and Gunn, 2018). Because of this, abnormal increases in Aβ for A- individuals can be measured more accurately, allowing for the determination of a subthreshold A+ cutoff (Zammit et al., 2021). In addition, $A\beta_L$ obtains information from all Aβ-carrying voxels in the brain rather than from a select number of ROIs, providing an estimate of the true global Aβ burden.

The progression of neurofibrillary tau accumulation and its relationship to Aβ and cognitive decline has been of recent interest. The emergence of tau PET radiotracers, such as flortaucipir (7-(6-(18F)fluoropyridin-3-yl)-5H-pyrido[4,3-b]indole, [F-18]AV-1451) (Xia et al., 2013), allows for an *in vivo* measurement of the degree and spatial extent of tau deposition. Early tau PET studies in late-onset Alzheimer's disease have shown that the spatial progression of PET-detectable tau tracks closely with the sequence of progression of tau pathology described in the classic studies of Braak and Braak (Lowe et al., 2018; Braak and Braak, 1997), that tau is highly associated with Aβ deposition and cognitive decline (Brier et al., 2016), and that tau PET can distinguish different clinical groups in the Alzheimer's disease continuum (Johnson et al., 2016). In late-onset Alzheimer's disease, tau PET has been shown to be more closely associated than Aβ PET with cognitive decline and dementia status (Ossenkoppele et al., 2016). However, these studies primarily focus on evaluation of individuals with high tau burden where cognitive decline is already present. Less emphasis has been placed on the detection of tau in early stage, presymptomatic disease where intervention may be more effective at preventing cognitive decline and neurodegeneration.

While tau PET has rapidly been adapted for use in late-onset Alzheimer's disease research studies, its use in Down syndrome has been understudied. Tau PET investigations in Down syndrome have demonstrated that increased tau burden is very highly correlated with cognitive impairment (Rafii et al., 2017) and that tau deposition in Braak stage regions III-VI accelerates with increasing Aβ deposition (Tudorascu et al., 2020). A recent study in Down syndrome has shown elevated levels of phospho-tau in cerebrospinal fluid in the fourth decade of life, directly following increases in Aβ PET (Fortea et al., 2020). Similar to late-onset Alzheimer's disease studies, evaluation of tau in Down syndrome has primarily focused on individuals with high Aβ and tau burden, with little emphasis on early tau detection. To date, no PET studies in Down syndrome have focused on detection of early tau in relation to early Aβ progression.

The Alzheimer's Biomarker Consortium – Down Syndrome (ABC-DS) is an ongoing longitudinal study with a large cohort aimed at characterizing the progression of Alzheimer's disease-related biomarker change in individuals with Down syndrome (Handen et al., 2020). The objectives of the current study were to assess neurofibrillary tau burden using AV-1451 PET and to compare Braak regional tau deposition to global Aβ. Using groups of A−, subthreshold A+ and conventionally A+ individuals with Down syndrome, regional AV-1451 was assessed to identify the earliest detectable increases in neurofibrillary tau. In an effort to identify and characterize the earliest detectable changes in PET-measured neurofibrillary tau and the relationship with Aβ, this investigation will expand upon the previous findings from ABC-DS by focusing on the deposition of neurofibrillary tau in individuals with very low levels of Aβ burden.

2. Materials and Methods

2.1. Participants

The current sample included 161 adults with Down syndrome (mean age (SD) = 39.2 (8.50) years) recruited by the University of Wisconsin-Madison, University of Pittsburgh, University of Cambridge, and Barrow Neurological Institute sites of the ABC-DS study (Handen et al., 2020). Institutional Review Board approval and informed consent were obtained during enrollment into the study by the participant or legally designated caregiver according to the Declaration of Helsinki. Inclusion criteria involved being aged ≥ 25 years and having a receptive language mental age of at least three years, based upon the Peabody Picture Vocabulary Test Fourth Edition (PPVT) (Dunn and Dunn, 2007). Genetic testing was performed to confirm Down syndrome (trisomy 21,

mosaicism, or partial translocation). Exclusion criteria included having an unstable psychiatric condition (e.g. untreated) that impaired cognitive functioning or a medical condition that was contraindicative of brain imaging scans (e.g. metallic implants). In the current study, eight participants were classified having Alzheimer's disease, eight were classified having mild cognitive impairment, 137 were cognitively stable, and the remaining eight showed cognitive decline but possibly due to non-Alzheimer's disease reasons (e.g., life stressors or medical conditions). Determination of cognitively stable status was based on consensus process that involved review of caregiver-reported and directly-administered measures of cognition and adaptive behavior and was made in consideration of premorbid intellectual disability level, psychiatric and medical conditions and major life events (Hartley et al., 2020). These diagnostic classifications were performed independent of imaging findings and based on case consensus processing informed by directly administered and caregiver-reported measures as previously described (Handen et al., 2020). Participant demographics are outlined in Table 1.

Additionally, 40 sibling controls (43.2 (12.6) years) without Down syndrome were enrolled in the study to act as a biomarker reference group. The control group was age-matched to the participants with Down syndrome and were determined to be free of symptoms of dementia based on the Montreal Cognitive Assessment (Nasreddine et al., 2005) and the Eight-Item Interview to Differentiate Aging and Dementia (Galvin et al., 2005, 2006). The control group underwent the same imaging protocols as the participants with Down syndrome but were not administered any additional cognitive testing or neurological examinations.

2.2. Sociodemographics

Chronological age was coded in years and sex was coded as M/F as reported by caregivers. The Peabody Picture Vocabulary Test – Fourth Edition (PPVT) (Dunn and Dunn, 2007) was administered to assess lifetime cognitive ability. The PPVT has been shown to be a valid measure of receptive language in adults with Down syndrome that highly correlates with IQ (Phillips et al., 2014).

2.3. Imaging

T1-weighted magnetic resonance imaging (MRI) scans were acquired on a GE Discovery MR750 (Wisconsin), Siemens Trio or Prisma (Pittsburgh), GE SIGNA (Cambridge), and GE Discovery MR750 (Barrow). MRI images were processed using FreeSurfer v5.3.0 for region of interest (ROI) definition. Positron emission tomography (PET) scans were performed on a Siemens ECAT HR + scanner (Wisconsin/Pittsburgh), Siemens 4-ring Biograph mCT (Pittsburgh), GE SIGNA (Cambridge), and GE Discovery 710 (Barrow). A target dose of 15 mCi of [C-11]Pittsburgh Compound-B (PiB) was injected intravenously, and PET scans were used to measure Aβ acquired 50–70 min post-injection (four 5-minute frames). Following completion of the PiB scan, a target dose of 10 mCi of [F-18]AV-1451 was injected intravenously, and PET scans were used to measure neurofibrillary tau acquired 80–100 min post-injection (four 5-minute frames). Using the Statistical Parametric Mapping 12 software (SPM12), PET frames were re-aligned to correct for motion and averaged to form a 3D image.

Table 1
Down syndrome participant demographics categorized by Aβ status.

	All	A-	Subthreshold A+	A+
Number of participants	**161**	108	22	31
Sex (M/F)	**81/80**	52/56	11/11	18/13
Chronological age (years)	**39.2 (8.50)**	34.9 (5.64)	44.4 (6.32)	50.4 (4.70)
PPVT mental age (years)	**9.83 (3.07)**	10.2 (2.90)	10.0 (3.07)	8.49 (3.23)
Mild cognitive impairment/ Alzheimer's disease consensus	**16**	1	1	14

2.4. Aβ PET quantification

PiB PET images were spatially normalized to the Montreal Neurological Institute 152 space (MNI152) via a Down syndrome-specific PET template for PiB as previously described (Lao et al., 2018). For all images, spatial normalization was required to calculate the amyloid load ($A\beta_L$) (Whittington and Gunn, 2018); a global measure of Aβ burden calculated from the linear least squares method between the PET image and images of specific and nonspecific PiB binding defined in MNI152 space. Standardized uptake value ratio (SUVr) images were generated by voxel normalization to cerebellar gray matter, and the global $A\beta_L$ was calculated following methodology specific to Down syndrome PiB images as previously described (Zammit et al., 2020). Because the striatum is a region of interest in the monitoring of early Alzheimer's disease progression in Down syndrome, striatal PiB SUVr was also calculated for each participant. Participants were classified as Aβ-negative (A-) for $A\beta_L < 13.3$ (Centiloid < 18.0), subthreshold A+ for $13.3 \leq A\beta_L < 20$ ($18.0 \leq$ Centiloid < 33.3), and conventionally A+ for $A\beta_L \geq 20$ (Centiloid ≥ 33.3). The conventional A+ cutoff was derived in Down syndrome by linearly transforming a previously established SUVr/Centiloid cutoff for A+ into units of $A\beta_L$ (Zammit et al., 2020). The cutoff for subthreshold A+ was derived from a longitudinal analysis that distinguished early Aβ accumulators from non-accumulators prior to surpassing the conventional A+ cutoff (Zammit et al., 2021). The conversion from $A\beta_L$ to Centiloids is as follows:

$$Centiloid = 2.27 * A\beta_L - 12.1 \quad (1)$$

Because these two metrics are very highly correlated at the cross-sectional level, an individual's group assignment would not change if Centiloids were used for classification instead of $A\beta_L$.

2.5. Tau PET quantification

AV-1451 PET images were coregistered to the T1w-MRI for the Down syndrome and sibling control participants. SUVr images were generated by voxel normalization to cerebellar gray matter and regional SUVrs were extracted from Braak regions I-VI (Schöll et al., 2016), with the exception that the striatum was not included in Braak region V. No erosion or elimination of regions of focal uptake of AV-1451 was performed on the cerebellar gray matter ROI used for signal normalization. Briefly, the T1w-MRI were processed using FreeSurfer v5.3.0 to delineate anatomical ROI masks for multiple brain regions. ROI masks from FreeSurfer were combined to create Braak stage ROIs, which were used to calculate the average AV-1451 SUVr within each Braak region. SUVr images were partial volume corrected using the geometric transfer matrix (GTM) method (Rousset et al., 1998), which has shown to be an effective method of reducing spillover effects from the choroid plexus in AV-1451 images (Baker et al., 2017). Quantification from non-PVC SUVr images was used for Braak regions III-VI, but due to AV-1451 off-target binding concerns in the choroid plexus, quantification from GTM-PVC results was used for Braak regions I-II. The mean SUVr values and standard deviations were calculated for each Braak region in the sibling control group and were used to compute a "control-standardized SUVr" score for the participants with Down syndrome. The control-standardized SUVr is a type of Z-score, but instead of being standardized to the mean and the distribution of the Down syndrome population, it is standardized to the mean and the distribution of the sibling control population. This provides the advantage of interpreting these derived scores in terms of how low/high the Down syndrome group is relative to the sibling controls. The T1w-MRI were then spatially normalized to the MNI152 space using SPM12, and the resulting deformation fields were

used to spatially normalize the AV-1451 SUVr images.

2.6. Statistical analyses

All statistical analyses were performed using SAS 9.4. Global $A\beta_L$ and Braak regional AV-1451 control-standardized SUVrs were compared using Pearson's partial correlations while adjusting for age, PPVT, and imaging site. For Braak regions I-II, the Pearson's partial correlations were also adjusted for AV-1451 in the choroid plexus. The Pearson's analysis was then repeated to compare striatal PiB SUVr to Braak regional control-standardized SUVr. AV-1451 control-standardized SUVrs across all Braak regions were then compared across groups of A-, subthreshold A+, and A+ individuals with Down syndrome using analysis of covariance (ANCOVA) while adjusting for age, PPVT and imaging site. For Braak regions I-II, the ANCOVA analysis also included AV-1451 in the choroid plexus as a covariate. Individual group comparisons were then performed by taking the least square differences between the means while adjusting for multiple comparisons using the Tukey-Kramer method. Group-averaged AV-1451 images (MNI152 space) were then generated for the A- and subthreshold A+ groups, and the difference was taken between the images to visualize regional differences in AV-1451 retention. Because the mean age of the subthreshold A+ group was ~10 years older than the A- group, an additional analysis was performed with an age-matched sample of the A- and subthreshold A+ groups to account for age-related effects. Using an age-matched sample of A- and subthreshold A+ Down syndrome, Braak regional AV-1451 control-standardized SUVrs were compared using two-tailed Student's t-tests while adjusting for imaging site. For Braak regions I-II, all comparisons were made both with and without GTM correction.

2.7. Data availability

The imaging sites have entered web-based data through the Alzheimer's Therapeutic Research Institute (ATRI) as part of the ABC-DS study. Data from the ABC-DS study and research methodology is currently available to the scientific community through the LONI database.

3. Results

3.1. Global $A\beta_L$, striatal PiB SUVr and Braak regional AV-1451

In this cohort, 108 individuals with Down syndrome were classified as A-, 22 were subthreshold A+, and 31 were conventionally A+. Representative AV-1451 SUVr images showing elevated binding in each Braak region are displayed in Fig. 1. Average AV-1451 SUVr images for the A-, subthreshold A+ and conventionally A+ groups are displayed in Fig. 2. Fig. 3 displays the AV-1451 control-standardized SUVr with respect to global $A\beta_L$ for each individual Braak region. Pearson's partial correlations (presented as Pearson's R [95% CI]) revealed significant positive associations (all $p < .0001$) with a large magnitude effect size (Cohen's d) (Cohen, 1988, 1992) between $A\beta_L$ and AV-1451 in all Braak regions (Braak I: 0.70 [0.61, 0.77]; Braak II: 0.74 [0.66, 0.81]; Braak III: 0.83 [0.77, 0.87]; Braak IV: 0.79 [0.72, 0.84]; Braak V: 0.81 [0.75, 0.86]; Braak VI: 0.77 [0.70, 0.83]). Following GTM correction, significant associations between $A\beta_L$ and AV-1451 remained significant in Braak regions I (0.56 [0.44, 0.66]) and II (0.56 [0.44, 0.66]). Pearson's partial correlations were then performed between striatal PiB SUVr and Braak regional AV-1451. Positive associations were observed between striatal PiB and AV-1451 in all Braak regions (Braak I: 0.65 [0.55, 0.74]; Braak II: 0.66 [0.56, 0.74]; Braak III: 0.63 [0.52, 0.72]; Braak IV: 0.58 [0.46, 0.68]; Braak V: 0.58 [0.46, 0.68]; Braak VI: 0.51 [0.38, 0.62]). Following GTM correction, significant associations between striatal PiB and AV-1451 remained significant in Braak regions I (0.55 [0.42, 0.66]) and II (0.50 [0.37, 0.61]). All associations survived adjustment for age, PPVT, and imaging site. In addition, the associations for Braak regions I-II survived adjustment for AV-1451 in the choroid plexus.

3.2. AV-1451 retention relative to $A\beta$ status

From ANCOVA, significant differences in AV-1451 control-standardized SUVr were observed between the A-, subthreshold A+, and A+ groups for Braak regions I ($F(df) = 23.4(6)$, $p < .0001$), II ($F(df) = 40.4(6)$, $p < .0001$), III ($F(df) = 32.8(5)$, $p < .0001$), IV ($F(df) = 22.7(5)$, $p < .0001$), V ($F(df) = 17.9(5)$, $p < .0001$), and VI ($F(df) = 10.6(5)$, $p < .0001$). Additionally, significant differences were observed following

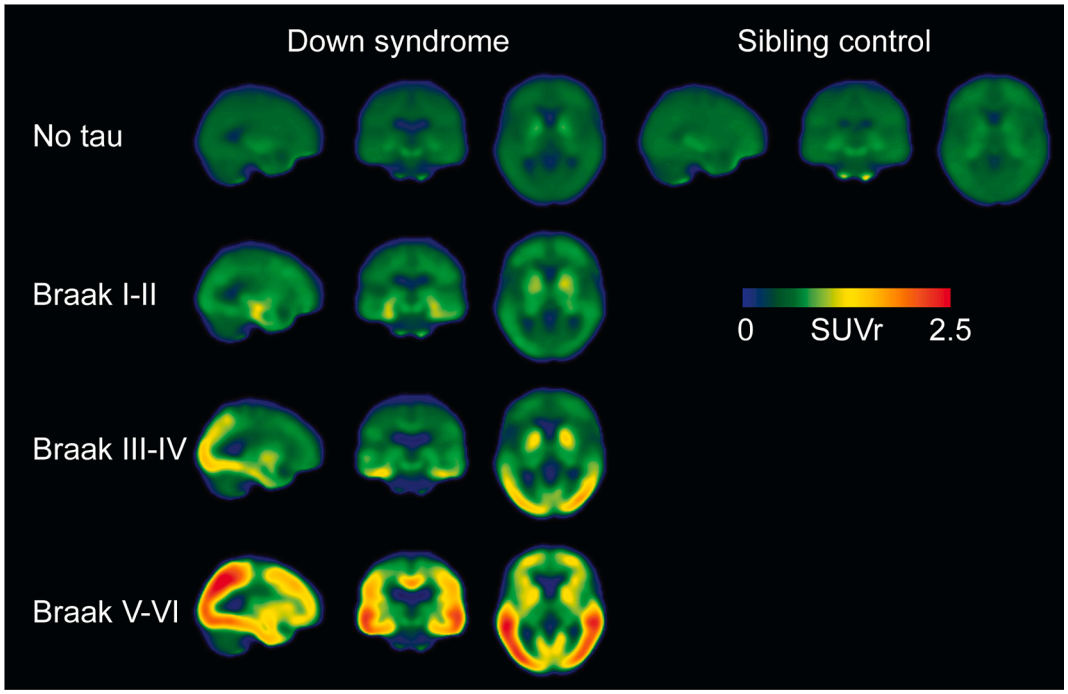

Fig. 1. Representative AV-1451 images for individuals with Down syndrome across each Braak stage, and for the sibling controls.

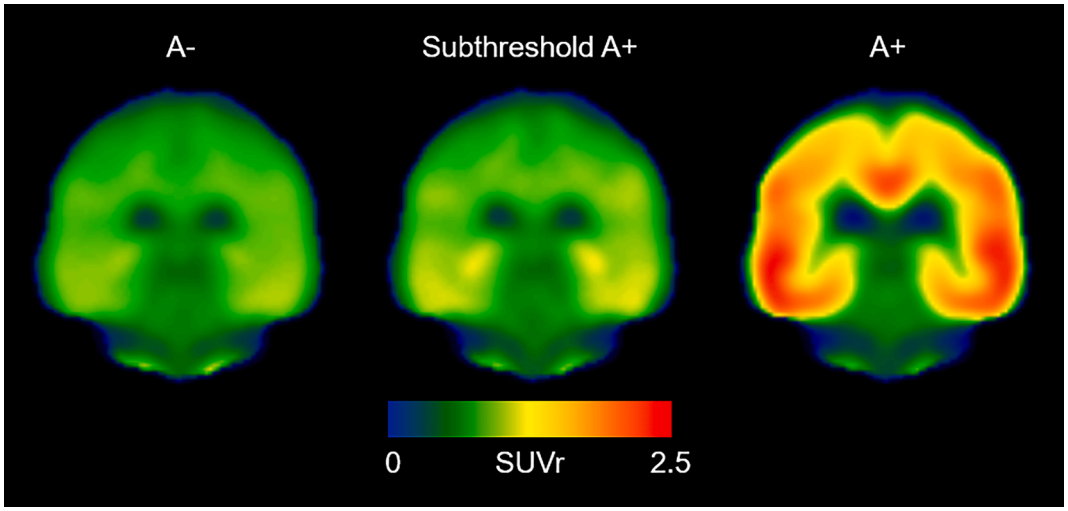

Fig. 2. Average AV-1451 SUVr images for groups of A-, subthreshold A+ and conventionally A+ individuals with Down syndrome.

GTM correction in Braak regions I ($F(df) = 14.8(6)$, $p < .0001$) and II ($F(df) = 24.7(6)$, $p < .0001$). All associations survived adjustment for age, PPVT and imaging site. The associations for Braak regions I-II also survived adjustment for AV-1451 in the choroid plexus. From the individual group comparisons, least square differences between the means (with 95% CIs) for all Braak regions are displayed in Table 2. The A+ group showed significantly higher AV-1451 control-standardized SUVrs relative to the A- and the subthreshold A+ groups across Braak regions I-VI (all $p < .0001$ adjusted for multiple comparisons). The subthreshold A+ group showed significantly higher AV-1451 control-standardized SUVrs compared to the A- group in Braak regions I (adjusted $p = .0021$) and II (adjusted $p = .0031$) without GTM correction, and in Braak regions I (adjusted $p < .0001$) and II (adjusted $p = .0001$) with GTM correction. The subthreshold A+ group did not differ from the A- group in Braak regions III-VI (all $p > .05$ adjusted for multiple comparisons).

3.3. Age-matched comparison between AV-1451 retention for A- and subthreshold A+ groups

The SUVr difference image between the subthreshold A+ group-averaged and A- group-averaged AV-1451 images revealed higher retention in Braak regions I-III for the subthreshold A+ group (Fig. 4). Similarly, the SUVr difference image for age-matched samples of these groups revealed the same pattern of higher AV-1451 retention in Braak regions I-III in the subthreshold A+ group (Fig. 4). Using an age-matched sample of A- ($n = 72$) and subthreshold A+ ($n = 22$) individuals with Down syndrome, a Student's *t*-test analysis was performed to compare Braak regional AV-1451 retention between groups. AV-1451 control-standardized SUVrs were significantly higher in Braak regions I-III (all $p < .05$) for the subthreshold A+ group, and no significant difference was observed in Braak regions IV-VI between groups (Table 3). Imaging site did not influence the model outcome.

3.4. Discussion

Due to the similarities in Alzheimer's disease biomarker progression between Down syndrome and late-onset Alzheimer's disease, Down syndrome can serve as a model population for trials aimed at Alzheimer's disease prevention, such as those involving anti-amyloid treatments. Since the Down syndrome population is uniformly affected by Alzheimer's disease pathology during the fourth decade of life and progression of Alzheimer's disease biomarkers follow a predictable time course, recruitment of these individuals into projects such as the Trial-Ready Cohort – Down Syndrome (TRC-DS) study (Rafii et al., 2020) is more feasible compared to those at risk for late-onset Alzheimer's disease development. Our previous work in this population evaluated the longitudinal spread of Aβ (Zammit et al., 2021, 2020; Lao et al., 2017; Tudorascu et al., 2019), neurofibrillary tau deposition (Tudorascu et al., 2020), glucose hypometabolism (Lao et al., 2018; Zammit et al., 2020) and cognitive decline (Hartley et al., 2020) in order to characterize these biomarkers within the amyloid/tau/neurodegeneration (AT(N)) framework of Alzheimer's disease (Jack et al., 2016; Rafii et al., 2020). The current work builds upon these previous findings by evaluating neurofibrillary tau deposition during the earliest stages of Aβ accumulation in order to better characterize early tau progression. With a better characterization of early tau in relation to Aβ, clinical trial studies can utilize tau PET to evaluate whether an anti-amyloid therapy is effective at preventing tau progression, especially that tau is more strongly correlated with cognitive decline.

Using AV-1451 PET, we have shown that Braak regional tau in Down syndrome is highly associated with global Aβ burden measured using $A\beta_L$. The greatest associations between Aβ and tau were observed in Braak regions III-VI. In the A+ group, AV-1451 retention appeared to plateau with increased Aβ in Braak regions I-II, whereas Braak regions III-VI showed significantly increased tau burden. The lack of significant tau increase with Aβ in these early Braak regions is not unique to Down syndrome, as Braak I-II tau also appears to plateau while cortical regions continue to escalate in late-onset Alzheimer's disease (Jack et al., 2019; Schwarz et al., 2016). This may indicate that the associations between Aβ and tau in these early Braak regions are primarily driven by individuals with low to moderate Aβ burden, and that the positive association between biomarkers diminishes with higher Aβ levels. In a study of autosomal dominant Alzheimer's disease, striatal PiB showed greater associations with tau compared to cortical PiB (Hanseeuw et al., 2019), and it is suggested that striatal PiB may also be highly associated with regional tau spread in Down syndrome. To evaluate this, Pearson's partial correlations were performed between striatal PiB SUVr and Braak regional AV-1451 in our Down syndrome cohort. Striatal PiB SUVr was highly associated with Braak regional tau, however, the effect sizes were not as large when compared to global $A\beta_L$. The large effect sizes observed with $A\beta_L$ are likely a result of the improved sensitivity this metric provides to detect Aβ when compared to SUVr. Our previous work in Down syndrome reported significant associations between increased Aβ burden and cognition as well as associations between glucose hypometabolism and cognition (Zammit et al., 2020), and work is currently ongoing to evaluate the association of tau (treated as a continuous variable) across a range of cognitive domains.

While tau in Braak regions I-II had significant associations with Aβ,

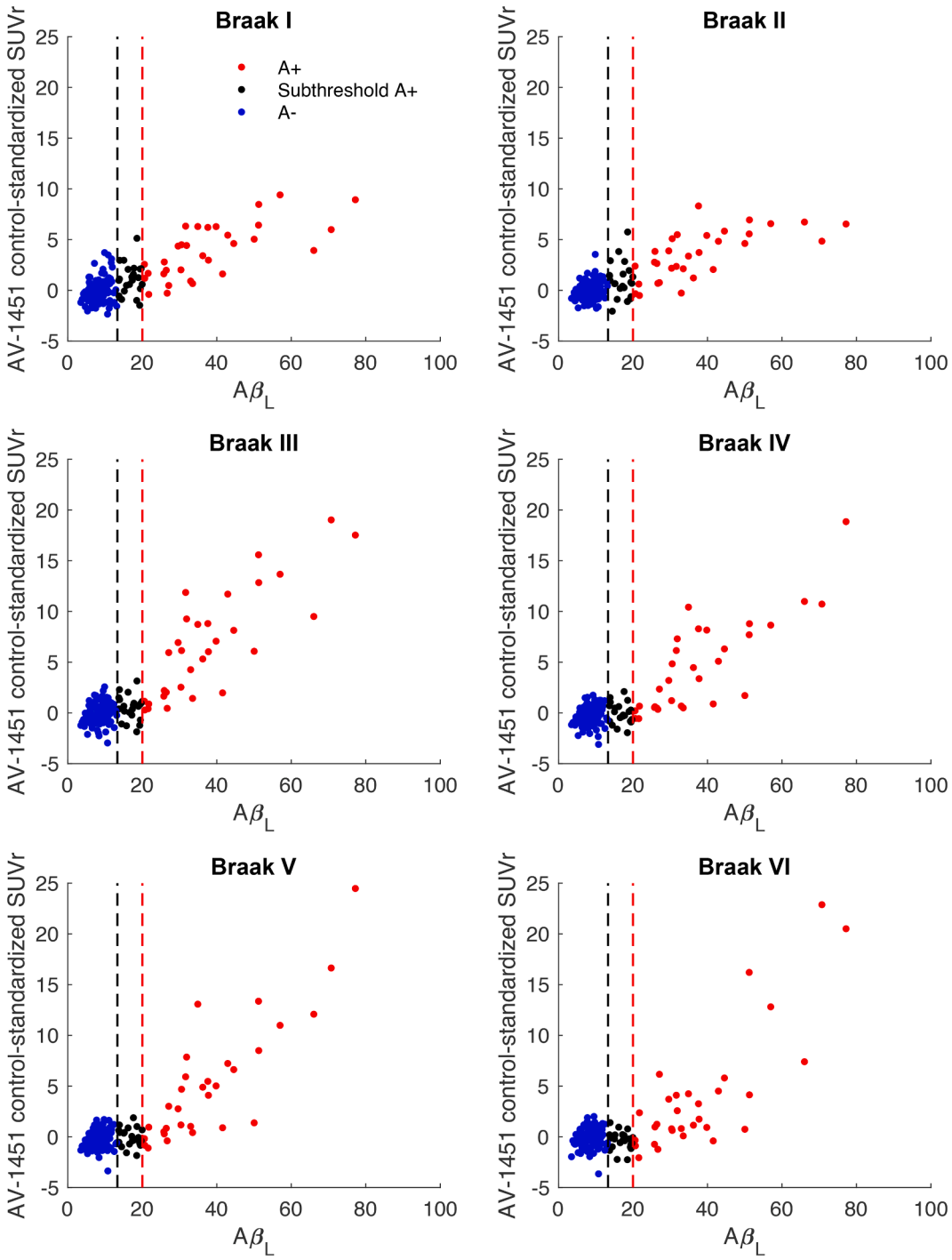

Fig. 3. Braak regional AV-1451 control-standardized SUVr with respect to global $A\beta_L$ for A-, subthreshold A+, and A+ Down syndrome.

the quantification of tau in these regions was likely influenced by signal spillover from off-target AV-1451 binding in the choroid plexus (Lois et al., 2019). To account for choroid plexus spillover, the geometric transfer matrix (GTM) method of partial volume correction was performed on Braak regions I-II. Following GTM correction, the associations between Aβ and tau remained significant in these regions. Due to off-target binding of AV-1451 in the basal ganglia, the striatum was excluded from Braak region V in these analyses. The voxel analysis evaluating SUVr difference images between subthreshold A+ and A− groups did reveal elevated striatal AV-1451 retention in the subthreshold A+ group, but when compared to an age-matched sample of A- individuals with Down syndrome, no difference was observed between striatal retention. This finding indicates that the striatal AV-1451 binding observed in Down syndrome may be age-related, similar to the patterns of increased AV-1451 retention in healthy controls with age (Smith et al., 2017). An AV-1451 study in frontotemporal dementia evaluated the potential of W-score maps (a modified Z-score adjusted for covariates) relative to a healthy control group to monitor increased retention while correcting for age-related effects (Tsai et al., 2019). Due to the association between age and off-target AV-1451 binding in the striatum, this methodology may be useful to distinguish Alzheimer's disease-related increases in striatal AV-1451 retention in Down syndrome. Because the striatum is a region of early Aβ deposition in Down syndrome, evaluation of the striatum with a radiotracer free from off-

Table 2
Least square differences (with 95% CIs) between the means of Braak regional AV-1451 control-standardized SUVr for A-, subthreshold A+, and A+ Down syndrome. Comparisons for Braak regions I-II were made without and with geometric transfer matrix (GTM) method partial volume correction.

Braak region	Group 1	Group 2	Least square difference [95% CI]
Braak I	A−	A+	−3.90 [−4.67, −3.13]****
	A−	Subthreshold A+	−1.23 [−2.09, −0.39]**
	Subthreshold A+	A+	−2.66 [−3.68, −1.64]****
Braak II	A−	A+	−3.62 [−4.30, −2.94]****
	A−	Subthreshold A+	−1.06 [−1.82, −0.31]**
	Subthreshold A+	A+	−2.56 [−3.46, −1.65]****
Braak I GTM	A−	A+	−3.30 [−4.20, −2.40]****
	A−	Subthreshold A+	−1.64 [−2.64, −0.65]***
	Subthreshold A+	A+	−1.65 [−2.86, −0.46]**
Braak II GTM	A−	A+	−2.11 [−2.57, −1.65]****
	A−	Subthreshold A+	−1.03 [−1.55, −0.53]***
	Subthreshold A+	A+	−1.07 [−1.68, −0.46]***
Braak III	A−	A+	−6.89 [−8.08, −5.69]****
	A−	Subthreshold A+	−0.68 [−2.00, 0.65]
	Subthreshold A+	A+	−6.21 [−7.80, −4.61]****
Braak IV	A−	A+	−4.85 [−5.90, −3.81]****
	A−	Subthreshold A+	−0.30 [−1.46, 0.85]
	Subthreshold A+	A+	−4.55 [−5.94, −3.16]****
Braak V	A−	A+	−5.44 [−6.75, −4.13]****
	A−	Subthreshold A+	−0.27 [−1.72, 1.18]
	Subthreshold A+	A+	−5.17 [−6.92, −3.43]****
Braak VI	A−	A+	−4.14 [−5.49, −2.79]****
	A−	Subthreshold A+	0.17 [−1.32, 1.67]
	Subthreshold A+	A+	−4.31 [−6.11, −2.52]****

Significance: * 0.05 ** 0.01 *** 0.001 **** 0.0001 adjusted for multiple comparisons using the Tukey-Kramer method.

target basal ganglia binding may better characterize tau spread in this region. Our findings also suggest that the spatial patterns of tau follow the conventional Braak staging of tau pathology, as elevated tau was not present within a late Braak region at the individual level without already being elevated in each antecedent region. These findings are in accordance with our previous findings in Down syndrome showing that higher tau pathology emerges in Braak stage regions as Aβ pathology increases, and that the associations between Aβ and tau are similar to late-onset Alzheimer's disease (Tudorascu et al., 2020).

When evaluating Braak regional tau across groups based on Aβ status, the conventionally A+ group had significantly higher tau burden in all Braak regions compared to the subthreshold A+ and A− groups. Compared to the A- group, the subthreshold A+ group had significantly higher tau deposition in Braak regions I-II. Because the mean age of the subthreshold A+ group was ~10 years older than the A- group, an additional analysis was performed using an age-matched sample from the A- group to account for age-related effects. Given the age-matched samples, tau burden in Braak regions I-III was significantly higher in the subthreshold A+ group compared to the A- group, suggesting that Aβ status rather than age is a better indicator of tau presence. These findings suggest that tau deposition in Down syndrome can be detected during the subthreshold Aβ accumulation phase, highlighting the importance of early detection and intervention of Alzheimer's disease biomarker progression. The identification of early tau with subthreshold Aβ accumulation is not unique to Down syndrome, as both elevated tau and worsening cognitive performance were accompanied by subthreshold Aβ in late-onset Alzheimer's disease (Hanseeuw et al., 2019). Another study in late-onset Alzheimer's disease reports that individuals with subthreshold Aβ had predictable neocortical tau spread within a 5 year period, followed shortly by cognitive decline (Leal et al., 2018). Furthermore, memory decline was observed with subthreshold Aβ accumulation in healthy, older adults at risk for Alzheimer's disease (Landau et al., 2018). Due to the similarities between Alzheimer's disease pathology progression in Down syndrome and late-onset Alzheimer's disease, individuals with Down syndrome with a subthreshold A+ classification should be more carefully evaluated for cognitive decline.

For this analysis, we chose to quantify tau using control-standardized SUVrs from the AV-1451 data relative to the sibling control group. Control-standardized SUVrs were used as this method standardizes the SUVr by accounting for the regional variance of AV-1451 binding (Vemuri et al., 2017). Because the control-standardized SUVr is a method of Z-transforming the AV-1451 data, the associations observed between groups in this study would be the same as those observed with non-standardized SUVr. There are benefits to using control-standardized SUVrs, as this method can facilitate head-to-head comparisons of imaging studies that utilize different populations and different tau radiotracers, and they can also be used to generate a standardized cutoff for tau-positivity (T+) that would theoretically be similar across all tau PET radiotracers (Villemagne et al., 2020). For the current study, control-standardized SUVrs provided the sensitivity to identify very early tau deposition during the subthreshold Aβ accumulation phase, and lay the groundwork for establishing a T+ cutoff for Down syndrome within the AT(N) classification scheme (Jack et al., 2016; Rafii et al., 2020).

Future work in this population will focus on further evaluation of Aβ, tau, and neurodegeneration throughout Alzheimer's disease progression. Additionally, cutoffs for T+ in Down syndrome will be explored and can be validated (Salvadó et al., 2019) against plasma or cerebrospinal fluid biomarkers of total tau and phospho-tau181 (Handen et al., 2020) or phospho-tau217 (Mattsson-Carlgren, et al., 2021) that have been collected as part of ABC-DS. Longitudinal imaging of tau is also needed to explore tau accumulation across the different stages of Alzheimer's disease progression. Comparisons of tau with changes in cognition will also be performed using established outcome measures of cognitive decline for Down syndrome (Hartley et al., 2020).

3.5. Conclusion

Evaluating PiB and AV-1451 PET in a large Down syndrome population revealed significant associations between Aβ deposition and Braak-regional tau deposition. The A+ Down syndrome group showed higher tau burden in Braak regions I-VI compared to the subthreshold A+ and A− Down syndrome groups. The subthreshold A+ group showed significantly higher tau burden in Braak regions I-III compared to an age-matched subset of the A− group, suggesting that tau deposition begins very early in the preclinical Alzheimer's disease phase.

Funding

This study is funded by the National Institute on Aging (NIA) grants [U01AG051406, R01AG031110, U54HD090256] and the National Institute for Child Health and Human Development (NICHD).

CRediT authorship contribution statement

Matthew D. Zammit: Conceptualization, Methodology, Writing - original draft. **Dana L. Tudorascu:** Methodology, Writing - review & editing. **Charles M. Laymon:** Writing - review & editing. **Sigan L.**

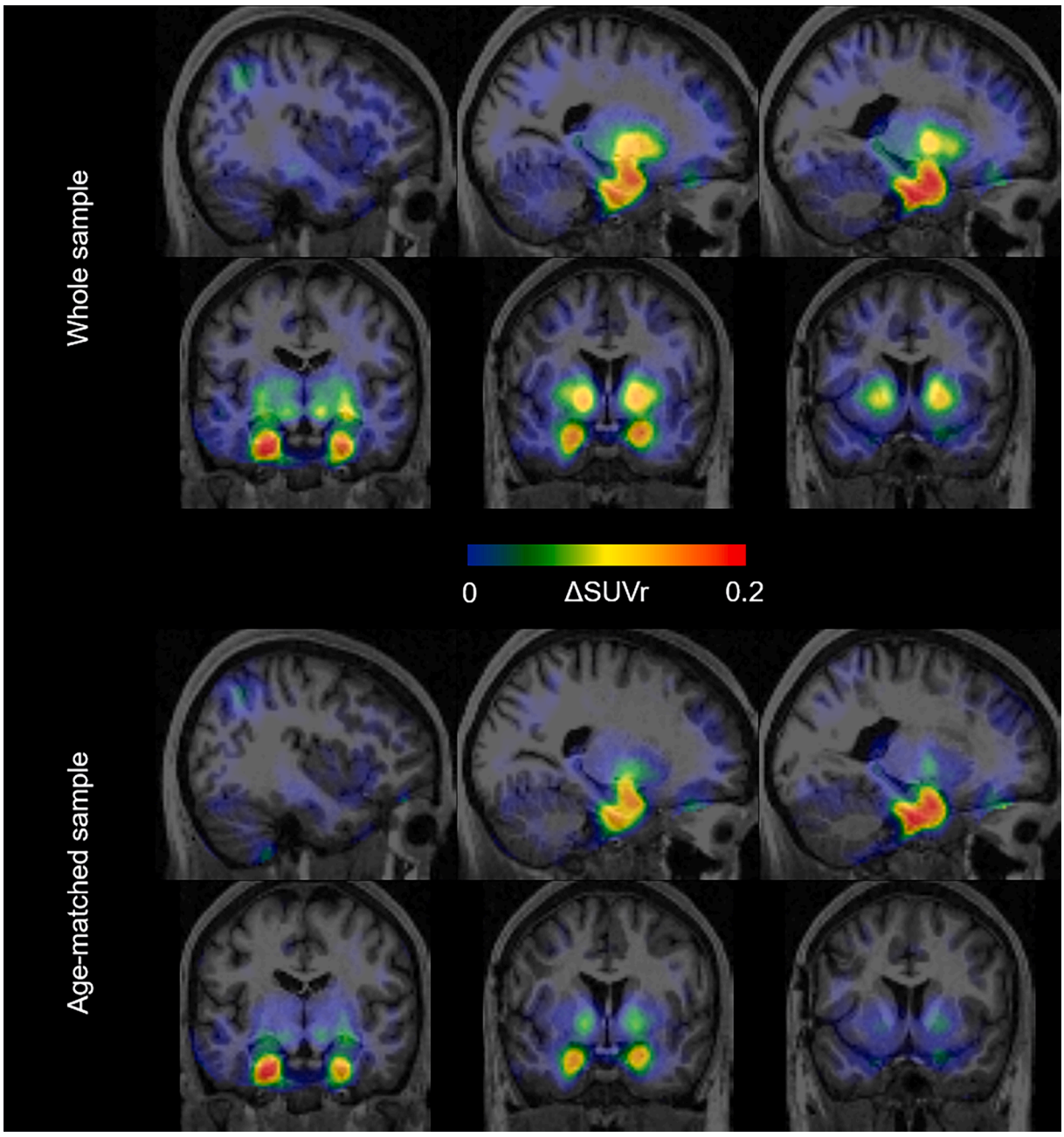

Fig. 4. Sagittal and coronal sections of AV-1451 SUVr difference images (ΔSUVr) between A- and subthreshold A+ adults with Down syndrome (top) and an age-matched sample of these individuals (bottom). Image slices are overlaid with a T1w-MRI from a healthy individual with Down syndrome warped into MNI152 space. Higher ΔSUVr in Braak regions I-III is indicative of elevated tau in the subthreshold A+ group.

Table 3
AV-1451 control-standardized SUVrs (with SDs) across each Braak region for groups of age-matched A- (N = 72) and subthreshold A+ (N = 22) adults with Down syndrome. Associations are adjusted for imaging site. Comparisons for Braak regions I-II were made without and with geometric transfer matrix (GTM) method partial volume correction.

Braak region	A-	Subthreshold A+	P-value
Braak I	0.085 (1.20)	1.12 (1.52)	0.0013
Braak II	0.048 (0.86)	1.01 (1.75)	0.0007
Braak I GTM	0.23 (1.72)	1.23 (2.13)	0.027
Braak II GTM	0.18 (0.75)	1.10 (1.52)	0.0002
Braak III	−0.033 (0.92)	0.50 (1.20)	0.030
Braak IV	−0.13 (0.81)	−0.033 (0.98)	0.61
Braak V	−0.15 (0.85)	−0.054 (0.89)	0.64
Braak VI	−0.15 (0.86)	−0.39 (0.89)	0.30

Hartley: Writing - review & editing. **Paul A. Ellison:** Writing - review & editing. **Shahid H. Zaman:** Writing - review & editing. **Beau M. Ances:** Writing - review & editing. **Sterling C. Johnson:** Writing - review & editing. **Charles K. Stone:** Writing - review & editing. **Marwan N. Sabbagh:** Writing - review & editing. **Chester A. Mathis:** Writing - review & editing. **William E. Klunk:** Funding acquisition, Writing - review & editing. **Ann D. Cohen:** Writing - review & editing. **Benjamin L. Handen:** Funding acquisition, Writing - review & editing. **Bradley T. Christian:** Funding acquisition, Supervision, Conceptualization, Writing - review & editing.

Declaration of Competing Interest

The authors declare that they have no known competing financial

interests or personal relationships that could have appeared to influence the work reported in this paper.

Acknowledgements

ABC-DS: The Alzheimer's Biomarkers Consortium – Down Syndrome (ABC-DS) project is a longitudinal study of cognition and blood based, genetic and imaging biomarkers of Alzheimer's Disease. We thank the ABC-DS study participants and the ABC-DS research and support staff for their contributions to this study.

This manuscript has been reviewed by ABC-DS investigators for scientific content and consistency of data interpretation with previous ABC-DS study publications. We acknowledge the ABC-DS study participants and the ABC-DS research and support staff for their contributions to this study. The content is solely the responsibility of the authors and does not necessarily represent the official views of the NIH.

References

Oyama, F., Cairns, N.J., Shimada, H., Oyama, R., Titani, K., Ihara, Y., 1994. Down's Syndrome: Up-Regulation of β-Amyloid Protein Precursor and τ mRNAs and Their Defective Coordination. Journal of Neurochemistry 62, 1062–1066. https://doi.org/10.1046/j.1471-4159.1994.62031062.x.

Rumble, B., Retallack, R., Hilbich, C., Simms, G., Multhaup, G., Martins, R., et al., 1989. Amyloid A4 Protein and Its Precursor in Down's Syndrome and Alzheimer's Disease. New England Journal of Medicine 320, 1446–1452. https://doi.org/10.1056/NEJM198906013202203.

Schupf, N., 2002. Genetic and host factors for dementia in Down's syndrome. The British Journal of Psychiatry 180, 405–410. https://doi.org/10.1192/bjp.180.5.405.

Strydom, A., Coppus, A., Blesa, R., Danek, A., Fortea, J., Hardy, J., et al., 2018. Alzheimer's disease in Down syndrome: An overlooked population for prevention trials. Alzheimer's & Dementia: Translational Research & Clinical Interventions 4, 703–713. https://doi.org/10.1016/j.trci.2018.10.006.

McCarron, M., McCallion, P., Reilly, E., Dunne, P., Carroll, R., Mulryan, N., 2017. A prospective 20-year longitudinal follow-up of dementia in persons with Down syndrome. Journal of Intellectual Disability Research 61, 843–852. https://doi.org/10.1111/jir.12390.

McCarron, M., McCallion, P., Reilly, E., Mulryan, N., 2014. A prospective 14-year longitudinal follow-up of dementia in persons with Down syndrome. Journal of Intellectual Disability Research 58, 61–70. https://doi.org/10.1111/jir.12074.

Sinai, A., Mokrysz, C., Bernal, J., Bohnen, I., Bonell, S., Courtenay, K., et al., 2018. Predictors of Age of Diagnosis and Survival of Alzheimer's Disease in Down Syndrome. Journal of Alzheimer's Disease 61, 717–728. https://doi.org/10.3233/JAD-170624.

Hithersay, R., Startin, C.M., Hamburg, S., Mok, K.Y., Hardy, J., Fisher, E.M.C., et al., 2019. Association of Dementia With Mortality Among Adults With Down Syndrome Older Than 35 Years. JAMA Neurol 76, 152. https://doi.org/10.1001/jamaneurol.2018.3616.

Handen, B.L., Cohen, A.D., Channamalappa, U., Bulova, P., Cannon, S.A., Cohen, W.I., et al., 2012. Imaging brain amyloid in nondemented young adults with Down syndrome using Pittsburgh compound B. Alzheimer's & Dementia 8, 496–501. https://doi.org/10.1016/j.jalz.2011.09.229.

Bateman, R.J., Xiong, C., Benzinger, T.L.S., Fagan, A.M., Goate, A., Fox, N.C., et al., 2012. Clinical and Biomarker Changes in Dominantly Inherited Alzheimer's Disease. New England Journal of Medicine 367, 795–804. https://doi.org/10.1056/NEJMoa1202753.

Klunk, W.E., Price, J.C., Mathis, C.A., Tsopelas, N.D., Lopresti, B.J., Ziolko, S.K., et al., 2007. Amyloid Deposition Begins in the Striatum of Presenilin-1 Mutation Carriers from Two Unrelated Pedigrees. J Neurosci 27, 6174–6184. https://doi.org/10.1523/JNEUROSCI.0730-07.2007.

Remes, A.M., Laru, L., Tuominen, H., Aalto, S., Kemppainen, N., Mononen, H., et al., 2008. Carbon 11–Labeled Pittsburgh Compound B Positron Emission Tomographic Amyloid Imaging in Patients With APP Locus Duplication. Arch Neurol 65, 540–544. https://doi.org/10.1001/archneur.65.4.540.

Villemagne, V.L., Ataka, S., Mizuno, T., Brooks, W.S., Wada, Y., Kondo, M., et al., 2009. High Striatal Amyloid β-Peptide Deposition Across Different Autosomal Alzheimer Disease Mutation Types. Arch Neurol 66, 1537–1544. https://doi.org/10.1001/archneurol.2009.285.

Annus, T., Wilson, L.R., Hong, Y.T., Acosta-Cabronero, J., Fryer, T.D., Cardenas-Blanco, A., et al., 2016. The pattern of amyloid accumulation in the brains of adults with Down syndrome. Alzheimer's & Dementia 12, 538–545. https://doi.org/10.1016/j.jalz.2015.07.490.

Cole, J.H., Annus, T., Wilson, L.R., Remtulla, R., Hong, Y.T., Fryer, T.D., et al., 2017. Brain-predicted age in Down syndrome is associated with beta amyloid deposition and cognitive decline. Neurobiology of Aging 56, 41–49. https://doi.org/10.1016/j.neurobiolaging.2017.04.006.

Hartley, S.L., Handen, B.L., Devenny, D.A., Hardison, R., Mihaila, I., Price, J.C., et al., 2014. Cognitive functioning in relation to brain amyloid-β in healthy adults with Down syndrome. Brain 137, 2556–2563. https://doi.org/10.1093/brain/awu173.

Jennings, D., Seibyl, J., Sabbagh, M., Lai, F., Hopkins, W., Bullich, S., et al., 2015. Age dependence of brain β-amyloid deposition in Down syndrome. Neurology 84, 500. https://doi.org/10.1212/WNL.0000000000001212.

Landt, J., D'Abrera, J.C., Holland, A.J., Aigbirhio, F.I., Fryer, T.D., Canales, R., et al., 2011. Using Positron Emission Tomography and Carbon 11–Labeled Pittsburgh Compound B to Image Brain Fibrillar β-Amyloid in Adults With Down Syndrome: Safety, Acceptability, and Feasibility. Arch Neurol 68, 890–896. https://doi.org/10.1001/archneurol.2011.36.

Lao, P.J., Handen, B.L., Betthauser, T.J., Cody, K.A., Cohen, A.D., Tudorascu, D.L., et al., 2018. Imaging neurodegeneration in Down syndrome: brain templates for amyloid burden and tissue segmentation. Brain Imaging and Behavior. https://doi.org/10.1007/s11682-018-9888-y.

Lao, P.J., Betthauser, T.J., Hillmer, A.T., Price, J.C., Klunk, W.E., Mihaila, I., et al., 2016. The effects of normal aging on amyloid-β deposition in nondemented adults with Down syndrome as imaged by carbon 11–labeled Pittsburgh compound B. Alzheimer's & Dementia 12, 380–390. https://doi.org/10.1016/j.jalz.2015.05.013.

Mak, E., Bickerton, A., Padilla, C., Walpert, M.J., Annus, T., Wilson, L.R., et al., 2019. Longitudinal trajectories of amyloid deposition, cortical thickness, and tau in Down syndrome: A deep-phenotyping case report. Alzheimer's & Dementia: Diagnosis, Assessment & Disease Monitoring 11, 654–658. https://doi.org/10.1016/j.dadm.2019.04.006.

Matthews, D.C., Lukic, A.S., Andrews, R.D., Marendic, B., Brewer, J., Rissman, R.A., et al., 2016. Dissociation of Down syndrome and Alzheimer's disease effects with imaging. Alzheimer's & Dementia: Translational Research & Clinical Interventions 2, 69–81. https://doi.org/10.1016/j.trci.2016.02.004.

Rafii, M., Wishnek, H., Brewer, J., Donohue, M., Ness, S., Mobley, W., et al., 2015. The down syndrome biomarker initiative (DSBI) pilot: proof of concept for deep phenotyping of Alzheimer's disease biomarkers in down syndrome. Front. Behav Neurosci 9. https://doi.org/10.3389/fnbeh.2015.00239.

Rafii, M.S., Lukic, A.S., Andrews, R.D., Brewer, J., Rissman, R.A., Strother, S.C., et al., 2017. PET Imaging of Tau Pathology and Relationship to Amyloid, Longitudinal MRI, and Cognitive Change in Down Syndrome: Results from the Down Syndrome Biomarker Initiative (DSBI). Journal of Alzheimer's Disease 60, 439–450. https://doi.org/10.3233/JAD-170390.

Sabbagh, M.N., Chen, K., Rogers, J., Fleisher, A.S., Liebsack, C., Bandy, D., et al., 2015. Florbetapir PET, FDG PET, and MRI in Down syndrome individuals with and without Alzheimer's dementia. Alzheimer's & Dementia 11, 994–1004. https://doi.org/10.1016/j.jalz.2015.01.006.

Lao, P.J., Handen, B.L., Betthauser, T.J., Mihaila, I., Hartley, S.L., Cohen, A.D., et al., 2017. Longitudinal changes in amyloid positron emission tomography and volumetric magnetic resonance imaging in the nondemented Down syndrome population. Alzheimer's & Dementia: Diagnosis, Assessment & Disease Monitoring 9, 1–9. https://doi.org/10.1016/j.dadm.2017.05.001.

Tudorascu, D.L., Anderson, S.J., Minhas, D.S., Yu, Z., Comer, D., Lao, P., et al., 2019. Comparison of longitudinal Aβ in nondemented elderly and Down syndrome. Neurobiology of Aging 73, 171–176. https://doi.org/10.1016/j.neurobiolaging.2018.09.030.

Zammit, M., Laymon, C.M., Betthauser, T.J., Cody, K.A., Tudorascu, D.L., Minhas, D.S., et al., 2020. Amyloid accumulation in Down syndrome measured with amyloid load. Alzheimer's & Dementia: Diagnosis, Assessment & Disease Monitoring 12, e12020. https://doi.org/10.1002/dad2.12020.

Hanseeuw, B.J., Betensky, R.A., Mormino, E.C., Schultz, A.P., Sepulcre, J., Becker, J.A., et al., 2018. PET staging of amyloidosis using striatum. Alzheimer's & Dementia. https://doi.org/10.1016/j.jalz.2018.04.011.

Cohen, J., 1992. Statistical power analysis. Current Directions in Psychological Science 1, 98–101.

Cohen, A.D., McDade, E., Christian, B., Price, J., Mathis, C., Klunk, W., et al., 2018. Early striatal amyloid deposition distinguishes Down syndrome and autosomal dominant Alzheimer's disease from late-onset amyloid deposition. Alzheimer's & Dementia 14, 743–750. https://doi.org/10.1016/j.jalz.2018.01.002.

Hanseeuw, B.J., Betensky, R.A., Jacobs, H.I.L., Schultz, A.P., Sepulcre, J., Becker, J.A., et al., 2019. Association of Amyloid and Tau With Cognition in Preclinical Alzheimer Disease: A Longitudinal Study. JAMA Neurol 76, 915. https://doi.org/10.1001/jamaneurol.2019.1424.

Landau, S.M., Horng, A., Jagust, W.J., 2018. Memory decline accompanies subthreshold amyloid accumulation. Neurology 90, e1452–e1460. https://doi.org/10.1212/WNL.0000000000005354.

Leal, S.L., Lockhart, S.N., Maass, A., Bell, R.K., Jagust, W.J., 2018. Subthreshold Amyloid Predicts Tau Deposition in Aging. J Neurosci 38, 4482–4489. https://doi.org/10.1523/JNEUROSCI.0485-18.2018.

Zammit, M.D., Tudorascu, D.L., Laymon, C.M., Hartley, S.L., Zaman, S.H., Ances, B.M., et al., 2021. PET measurement of longitudinal amyloid load identifies the earliest stages of amyloid-beta accumulation during Alzheimer's disease progression in Down syndrome. NeuroImage 228, 117728. https://doi.org/10.1016/j.neuroimage.2021.117728.

Xia, C.-F., Arteaga, J., Chen, G., Gangadharmath, U., Gomez, L.F., Kasi, D., et al., 2013. [18F]T807, a novel tau positron emission tomography imaging agent for Alzheimer's disease. Alzheimer's & Dementia 9, 666–676. https://doi.org/10.1016/j.jalz.2012.11.008.

Lowe, V.J., Wiste, H.J., Senjem, M.L., Weigand, S.D., Therneau, T.M., Boeve, B.F., et al., 2018. Widespread brain tau and its association with ageing. Braak stage and Alzheimer's dementia. Brain 141, 271–287. https://doi.org/10.1093/brain/awx320.

Braak, H., Braak, E., 1997. Frequency of Stages of Alzheimer-Related Lesions in Different Age Categories. Neurobiology of Aging 18, 351–357. https://doi.org/10.1016/S0197-4580(97)00056-0.

Brier, M.R., Gordon, B., Friedrichsen, K., McCarthy, J., Stern, A., Christensen, J., et al., 2016;8:338ra66.. Tau and Aβ imaging, CSF measures, and cognition in Alzheimer's disease. Sci Transl Med. https://doi.org/10.1126/scitranslmed.aaf2362.

Johnson, K.A., Schultz, A., Betensky, R.A., Becker, J.A., Sepulcre, J., Rentz, D., et al., 2016. Tau positron emission tomographic imaging in aging and early Alzheimer disease. Annals of Neurology 79, 110–119. https://doi.org/10.1002/ana.24546.

Ossenkoppele, R., Schonhaut, D.R., Schöll, M., Lockhart, S.N., Ayakta, N., Baker, S.L., et al., 2016. Tau PET patterns mirror clinical and neuroanatomical variability in Alzheimer's disease. Brain 139, 1551–1567. https://doi.org/10.1093/brain/aww027.

Tudorascu, D.L., Laymon, C.M., Zammit, M., Minhas, D.S., Anderson, S.J., Ellison, P.A., et al., 2020. Relationship of amyloid beta and neurofibrillary tau deposition in Neurodegeneration in Aging Down Syndrome (NiAD) study at baseline. Alzheimer's & Dementia: Translational Research & Clinical Interventions 6, e12096. https://doi.org/10.1002/trc2.12096.

Fortea, J., Vilaplana, E., Carmona-Iragui, M., Benejam, B., Videla, L., Barroeta, I., et al., 2020. Clinical and biomarker changes of Alzheimer's disease in adults with Down syndrome: a cross-sectional study. The Lancet 395, 1988–1997. https://doi.org/10.1016/S0140-6736(20)30689-9.

Whittington, A., Gunn, RN. Amyloid Load – a more sensitive biomarker for amyloid imaging. J Nucl Med 2018. doi: 10.2967/jnumed.118.210518.

Handen BL, Lott IT, Christian BT, Schupf N, OBryant S, Mapstone M, et al. The Alzheimer's Biomarker Consortium-Down Syndrome: Rationale and methodology. Alzheimer's & Dementia: Diagnosis, Assessment & Disease Monitoring 2020;12: e12065. 10.1002/dad2.12065.

Dunn, L.M., Dunn, D.M., 2007. Peabody picture vocabulary test, 4th ed. NCD Pearson, Inc., San Antonio, TX.

Hartley, S.L., Handen, B.L., Devenny, D., Tudorascu, D., Piro-Gambetti, B., Zammit, M.D., et al., 2020. Cognitive indicators of transition to preclinical and prodromal stages of Alzheimer's disease in Down syndrome. Alzheimer's & Dementia: Diagnosis, Assessment & Disease Monitoring 12, e12096. https://doi.org/10.1002/dad2.12096.

Nasreddine, Z.S., Phillips, N.A., Bédirian, V., Charbonneau, S., Whitehead, V., Collin, I., et al., 2005. The Montreal Cognitive Assessment, MoCA: A Brief Screening Tool For Mild Cognitive Impairment. Journal of the American Geriatrics Society 53, 695–699. https://doi.org/10.1111/j.1532-5415.2005.53221.x.

Galvin, J.E., Roe, C.M., Powlishta, K.K., Coats, M.A., Muich, S.J., Grant, E., et al., 2005. The AD8: A brief informant interview to detect dementia. Neurology 65, 559–564. https://doi.org/10.1212/01.wnl.0000172958.95282.2a.

Galvin, J.E., Roe, C.M., Xiong, C., Morris, J.C., 2006. Validity and reliability of the AD8 informant interview in dementia. Neurology 67, 1942–1948. https://doi.org/10.1212/01.wnl.0000247042.15547.eb.

Phillips, B.A., Loveall, S.J., Channell, M.M., Conners, F.A., 2014. Matching variables for research involving youth with Down syndrome: Leiter-R versus PPVT-4. Research in Developmental Disabilities 35, 429–438. https://doi.org/10.1016/j.ridd.2013.11.016.

Schöll, M., Lockhart, S.N., Schonhaut, D.R., O'Neil, J.P., Janabi, M., Ossenkoppele, R., et al., 2016. PET Imaging of Tau Deposition in the Aging Human Brain. Neuron 89, 971–982. https://doi.org/10.1016/j.neuron.2016.01.028.

Rousset, O.G., Ma, Y., Evans, A.C., 1998. Correction for partial volume effects in PET: Principle and validation. Journal of Nuclear Medicine 39, 904–911.

Baker, S.L., Maass, A., Jagust, W.J., 2017. Considerations and code for partial volume correcting [18F]-AV-1451 tau PET data. Data in Brief 15, 648–657. https://doi.org/10.1016/j.dib.2017.10.024.

Cohen, J., 1988. Statistical power analysis for the behavioral sciences, 2nd ed. L. Erlbaum Associates, Hillsdale, N.J.

Rafii MS, Zaman S, Handen BL. Integrating Biomarker Outcomes into Clinical Trials for Alzheimer's Disease in Down Syndrome. J Prev Alzheimers Dis 2020. 10.14283/jpad.2020.35.

Lao, P.J., Handen, B.L., Betthauser, T.J., Mihaila, I., Hartley, S.L., Cohen, A.D., et al., 2018. Alzheimer-Like Pattern of Hypometabolism Emerges with Elevated Amyloid-β Burden in Down Syndrome. J Alzheimers Dis 61, 631–644. https://doi.org/10.3233/JAD-170720.

Zammit, M.D., Laymon, C.M., Tudorascu, D.L., Hartley, S.L., Piro-Gambetti, B., Johnson, S.C., et al., 2020. Patterns of glucose hypometabolism in Down syndrome resemble sporadic Alzheimer's disease except for the putamen. Alzheimer's & Dementia: Diagnosis, Assessment & Disease Monitoring 12, e12138. https://doi.org/10.1002/dad2.12138.

Jack, C.R., Bennett, D.A., Blennow, K., Carrillo, M.C., Feldman, H.H., Frisoni, G.B., et al., 2016. A/T/N: An unbiased descriptive classification scheme for Alzheimer disease biomarkers. Neurology 87, 539–547. https://doi.org/10.1212/WNL.0000000000002923.

Rafii, M.S., Ances, B.M., Schupf, N., Krinsky-McHale, S.J., Mapstone, M., Silverman, W., et al., 2020. The AT(N) framework for Alzheimer's disease in adults with Down syndrome. Alzheimer's & Dementia: Diagnosis, Assessment & Disease Monitoring 12, e12062. https://doi.org/10.1002/dad2.12062.

Jack Jr, C.R., Wiste, H.J., Botha, H., Weigand, S.D., Therneau, T.M., Knopman, D.S., et al., 2019. The bivariate distribution of amyloid-β and tau: relationship with established neurocognitive clinical syndromes. Brain 142, 3230–3242. https://doi.org/10.1093/brain/awz268.

Schwarz, A.J., Yu, P., Miller, B.B., Shcherbinin, S., Dickson, J., Navitsky, M., et al., 2016. Regional profiles of the candidate tau PET ligand 18 F-AV-1451 recapitulate key features of Braak histopathological stages. Brain 139, 1539–1550. https://doi.org/10.1093/brain/aww023.

Hanseeuw, B.J., Lopera, F., Sperling, R.A., Norton, D.J., Guzman-Velez, E., Baena, A., et al., 2019. Striatal amyloid is associated with tauopathy and memory decline in familial Alzheimer's disease. Alz Res Therapy 11, 17. https://doi.org/10.1186/s13195-019-0468-1.

Lois, C., Gonzalez, I., Johnson, K.A., Price, J.C., 2019. PET imaging of tau protein targets: a methodology perspective. Brain Imaging and Behavior 13, 333–344. https://doi.org/10.1007/s11682-018-9847-7.

Smith, R., Schain, M., Nilsson, C., Strandberg, O., Olsson, T., Hägerström, D., et al., 2017. Increased basal ganglia binding of 18 F-AV-1451 in patients with progressive supranuclear palsy. Mov Disord 32, 108–114. https://doi.org/10.1002/mds.26813.

Tsai, R.M., Bejanin, A., Lesman-Segev, O., LaJoie, R., Visani, A., Bourakova, V., et al., 2019. 18F-flortaucipir (AV-1451) tau PET in frontotemporal dementia syndromes. Alz Res Therapy 11, 13. https://doi.org/10.1186/s13195-019-0470-7.

Vemuri, P., Lowe, V.J., Knopman, D.S., Senjem, M.L., Kemp, B.J., Schwarz, C.G., et al., 2017. Tau-PET uptake: Regional variation in average SUVR and impact of amyloid deposition. Alzheimer's & Dementia: Diagnosis, Assessment & Disease Monitoring 6, 21–30. https://doi.org/10.1016/j.dadm.2016.12.010.

Villemagne, V.L., Lopresti, B.J., Dore, V., Tudorascu, D., Ikonomovic, M.D., Burnham, S., et al., 2020. What is T+? A Gordian Knot of Tracers, Thresholds & Topographies. Journal of Nuclear Medicine. https://doi.org/10.2967/jnumed.120.245423.

Salvadó, G., Molinuevo, J.L., Brugulat-Serrat, A., Falcon, C., Grau-Rivera, O., Suárez-Calvet, M., et al., 2019. Centiloid cut-off values for optimal agreement between PET and CSF core AD biomarkers. Alzheimer's Research & Therapy 11, 27. https://doi.org/10.1186/s13195-019-0478-z.

Mattsson-Carlgren N, S J, R B, R S, E S, G S, et al. Soluble P-tau217 reflects amyloid and tau pathology and mediates the association of amyloid with tau 2021. 10.21203/rs.3.rs-101153/v2.